Chemical Process Design Vol.1 No.2 (2022) 1-12

University of Sistan and Baluchestan

Chemical Process Design

Available online at http://cpd.usb.ac.ir/

Investigating Bubble Frequency Changes in Pool Boiling in Pure Solutions and on a Stainless Steel Cylinder

Samane Hamzekhani*, Mohammad Rasoul Kamalizade

Department of Chemical Engineering, University of Sistan and Baluchestan, Zahedan, Iran

ARTICLE INFO

Article history:
Received: 2022-10-19
Received in revised form: 2022-11-24
Accepted: 2022-12-07
Published online: 2022-12-07

Keywords:
Heat transfer; Saturated pool boiling; Pure liquid; Bubble departure; Frequency

DOI: *10.22111/CPD.2022.43741.1012*

ABSTRACT

Bubble dynamics is the most important sub-phenomenon, which basically affects the nucleate pool boiling heat transfer coefficient which includes bubble departure frequency, bubble diameter and nucleation site density. In this research, bubble departure frequency values were experimentally measured for heat fluxes up to 120 $kW.m^{-2}$. Experiments were carried out for pool boiling of pure liquids, including water, ethanol and methanol on a horizontal smoothed cylinder, at atmospheric pressure. A high-speed digital video camera was applied to capture the dynamics of the bubble nucleation process. For ethanol and methanol, rigid spherical bubbles with small contact area were observed. The spherical shapes seem to be because of small diameters. For all test fluids, experimental results show that the bubble frequency increase with increasing heat flux. Increase in the rate of bubble generation, reduction in the waiting time and growth time can be the causes of this phenomenon. Also, experimental results show, Heat transfer coefficient increases with increasing heat flux for all test fluids at the experimental condition.

1. Introduction

Nucleate boiling is a very efficient mode of heat transfer. It can be found in a wide range of applications in both traditional industries such as various energy conversion systems, heat exchange systems, air-conditioning, refrigeration and heat pump systems, chemical thermal processes and in highly specialized fields such as cooling of high-energy-density electronic components, micro-fabricated fluidic systems, the thermal control of aerospace stations, bioengineering reactors. The complete process of liquid heating, nucleation, bubble growth, and departure is the central mechanism of two-phase heat transfer from a superheated wall during nucleate pool boiling. Bubble frequencies f at detachment are of major importance to understand nucleate boiling heat transfer, and there are numerous experimental and theoretical studies on this. Bubble nucleation happens within the small activated cavities

Corresponding author. Tel.: +98 917 716 4806; fax: +98 (54) 33447231.
E-mail address: s.hamzekhani@usb.ac.ir (S. Hamzekhani).

at the heater surface when the wall temperature exceeds the saturation temperature of the liquid at the local pressure. Bubbles subsequently detach from the nucleation site due to the forces acting on them in the axial and radial directions. In spite of enormous efforts, bubble nucleation and departure phenomena in boiling are still considered as major challenges [1-10].

Bubble departure frequency can be deemed as the reciprocal of the summation of bubble waiting time (defined as the period from the moment that the former bubble departs to the moment that the current bubble nucleates) and bubble growth time (which is defined as the period from the moment of bubble appearance until the moment of bubble departure). The frequency of bubbles being released from cavities depends on multitude factors, including wall superheat, fluid physical properties, phase contact angle, cavity size, and interaction between neighboring bubbles. Because of the complex nature of this phenomenon, existing predictive correlations are developed based on different points of view. In the entire correlations, the bubble frequency is correlated to bubble diameter in various formats. This means that the prediction of bubble departure frequency is highly sensitive to bubble departure diameter and vice versa. The relations between f and d_b for an isolated bubble region in nucleate boiling are reported by Kim and Kim [11], Peebles and Garber [12], Zuber [13] and others. Many correlations are developed for the prediction of the bubble departure frequency for the nucleate pool boiling condition for different applications; the most important are summarized in Table 1.

Kim and Kim [11] conducted an experimental investigation of nucleate boiling heat transfer mechanism in pool boiling from wire heaters immersed in saturated FC-72 coolant and water. They have investigated the effects of the wire size on heat transfer mechanism during a nucleate boiling, varying 25 μm, 75 μm, and 390 μm, by measuring vapor volume flow rate and the frequency of bubbles departing from a wire immersed in saturated FC-72. Also, one wire diameter of 390 μm has been selected and tested in saturated water to investigate the fluid effect on the nucleate boiling heat transfer mechanism. Their experimental results show that the bubble frequency per unit wire area increases as the wire size decreases. They have concluded that since the perimeter of contact surface between the bubble and wire decreases as the wire size decreases, the buoyant force required to detach the bubbles for smaller size of wire relatively decreases compared to larger size of wire. Consequently, the bubble departure occurs with smaller volume of bubbles when the wire size decreases and this phenomenon provides the higher bubble frequency due to the reduced bubble growth time. In addition, their experimental data have shown that the average frequency per unit area for FC-72 stays fairly constant as heat flux increases. Also, dissimilarly with FC-72, all data points for water have shown a similar trend regardless of heat flux as the frequency of bubbles reduce with the increase of departing bubble size. McHale and Garimella [14] obtained quantitative measurements from high-speed visualizations of pool boiling at atmospheric pressure from smooth and roughened surfaces, using a perfluorinated hydrocarbon (FC-77) as the working fluid. The roughness values (Ra) have been reported 0.03 and 5.89 μm for the polished and roughened surfaces, respectively. The bubble diameter at departure, bubble departure frequency, active nucleation site density, and bubble terminal velocity have been measured from the monochrome movies, which have been recorded at 8000 frames per second with a digital CCD camera and magnifying lens. Their experimental results show that the values of bubble departure frequency for the polished surface are lower than for the roughened surface by as much as 47% for a given heat flux. Also, the authors have observed that both bubble departure frequency and diameter increase with heat flux and this increase has been much more pronounced for the polished surface. In

addition, they have reported that none of the departure frequency correlations seem applicable to the pool boiling of a Fluorinert and do not capture the trends seen in the experimental data.

Table 1. Correlations suggested for the prediction of bubble departure frequency

Researchers	Year	Correlation	Ref.
Model			
Jakob and Fritz(Kim and Kim)	2006	$fd = 0.078$	[11]
Peebles and Garber	1953	$fd_b = 1.18\left[\frac{t_g}{t_g + t_w}\right]\left[\frac{\sigma g_c g(\rho_l - \rho_v)}{\rho_l^2}\right]^{\frac{1}{4}}$	[12]
Zuber	1962	$f.d_b^{0.5} = 0.59[\frac{\sigma g(\rho_f - \rho_g)}{\rho_f^2}]^{\frac{1}{4}}$	[13]
Cole	1963	$f\ \frac{d_b^{0.5}}{g^{0.5}} = \sqrt{\frac{4(\rho_l - \rho_v)}{3\rho_l}}$	[15]
Hatton and Hall	1966	$f.d_b^2 = 0284.7\alpha_l$	[16]
McFadden and Grassman	1967	$f.d_b^{0.5} = 17.5\frac{cm^{0.5}}{s}$	[17]
Ivey	1967	$f.d_b^{0.75} = 0.44g^{0.5}cm^{0.25}$ $f.d_b^{0.5} = 0.9g^{0.5}$	[18]
Mikic and Rohsenow	1969	$f.d_b = \frac{4}{\pi}Ja\sqrt{3\pi\alpha_L}\left[[\frac{t_g}{t_g + t_w}]^{0.5} + [1 + \frac{t_g}{t_g + t_w}]^{0.5} - 1\right]$	[19]
Malenkov	1971	$fd_b = \frac{1}{\pi}\left(\frac{V_b}{1 - \frac{1}{1 + (V_b\rho_v h_{fg}/(q))}}\right)$ $V_b = \left[\frac{d_b g(\rho_l - \rho_v)}{2(\rho_l + \rho_v)} + \frac{2\sigma}{d_b(\rho_l + \rho_v)}\right]^{\frac{1}{2}}$	[20]
Stephan	1992	$f.d_b = \frac{1}{\pi}\sqrt{\frac{g}{2}(d_b + \frac{4\sigma}{\rho g d_d})}$	[21]

In the present study, an experimental investigation for the nucleate boiling heat transfer has been performed on a smooth horizontal cylinder immersed in saturated water, ethanol and methanol pure liquids at atmospheric pressure. The experimental results indicate a suitable overlap between the experimental data of bubble departure frequency and the values predicted by Stephan and Abdelsalam model. Data on the bubble departure frequency are measured and compared to the proposed correlations and models. It should be noted that predicting bubble frequency from the

proposed valid models requires calculation of parameters such as bubble diameter, bubble growth time and waiting time, which have their own complexities and limitations.

2. Experimental

2.1. Experimental setup

Fig. 1 schematically demonstrates the experimental equipment used in the present investigation. The cubic shaped boiling vessel is made of stainless steel containing approximately 20 L of test liquid and is connected to a vertical condenser to recycle the evaporated fluid. The assumptions related to saturation pool boiling condition hold true for this investigation due to the fact that the used boiling vessel has high volume relative to the boiling area and it is thermally insulated to minimize heat loss. System is continuously monitored and regulated to preserve predetermined operating condition. The saturation pressure (P = 1atm) is controlled by adjusting the mass flow rate of the cool water in the condensation loop. The water temperature and mass flow rate passing through the cooling coil are adjustable. Also, for safety reasons, a pressure relief valve is mounted on the top of the tank.

The vessel is equipped with two heaters: 1) auxiliary heater, which is a simple element to rise the bulk temperature to saturation temperature (P = 1atm), and 2) rod heater, which consists of an internally heated stainless steel rod equipped with four thermocouples stainless steel shielded and embedded along the circumference of the rod, close to the heating surface (0.75 mm). To minimize thermal contact resistance between each thermocouple and sheath, silicon paste is injected into the location of placing each thermocouple. Also, to minimize the influence of surface roughness on heat transfer, particularly on pool boiling heat transfer coefficient, the surface of the cylinder was polished using emery paper with an average roughness of 400 μm. The average roughness (Ra) of the test surface is measured by a portable surface roughness tester (TR200), and the value of Ra is 0.52 μm. The rod heater operates with variable A/C electrical power input providing variable heat fluxes. Details of the rod heater are given in Fig. 2. A PC-based data acquisition system was used to record some of the measuring parameters.

By means of two observation glasses positioned at both sides of the tank, the test section was easily observable, allowing ease of photography during the experiments. The electrical input power of the rod heater was calculated by the product of electrical voltage, current and cosine of the difference between input electrical voltage and current.

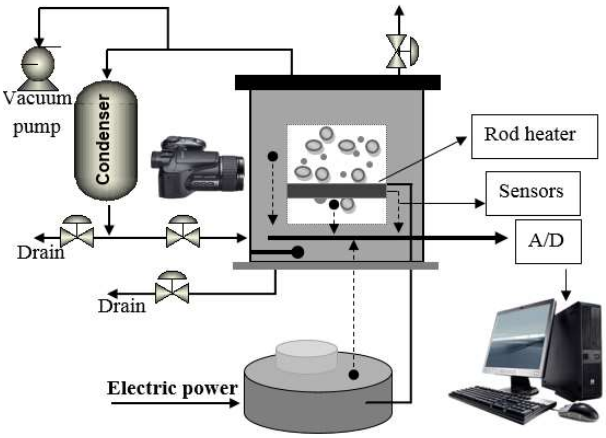

Fig. 1. Scheme of experimental apparatus used in this investigation

The temperature drop due to the existence of small distance between surface and thermocouple location was calculated by applying heat conduction equation for cylinders:

$$\frac{1}{r}\frac{d}{dr}(kr\frac{dT}{dr}) = 0 \quad (1)$$

In Eq. (1), k is the temperature dependent thermal conductivity of the heater, which was approximated to a linear function of temperature. The axial heat loss from the heated length to the unheated length of this rod was calculated to be less than 0.1 % of the total heat transfer [22]. The boiling heat transfer coefficient was calculated simply by Newton's cooling law and known value of wall temperature. Visual information related to bubbles was recorded by Casio EX-FH100 digital camera. This camera can record high-speed movies at 1,200 fps which is sufficient for the analysis of bubble motion. The typical photo specification was: shutter speed: 1:1000 s, ISO: 800, F: 5.5 and focal length: 100 mm (Approx). (With 10x zoom and technical specifications of Casio Exilim EX-FH100 fully compact such as 10KB optical zoom, optical image stabilization (CMOS Shift), integrated BSI CMOS image sensor (1/2.3 inch) JPEG and RAW (DNG) image format).

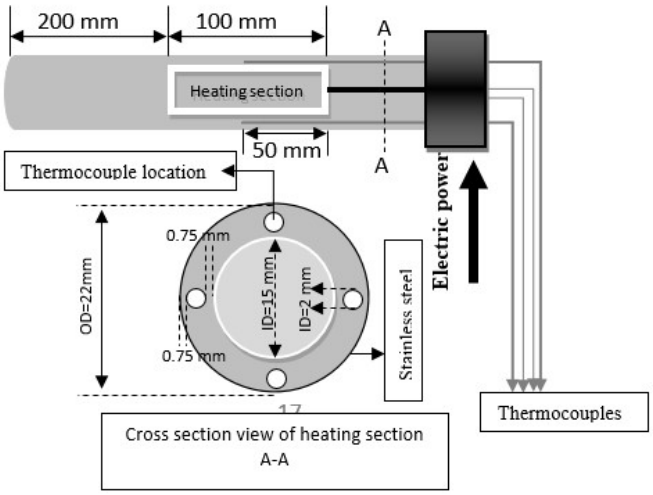

Fig. 2. Details of the rod heater

2.2. Procedure

The experiments have been entirely performed at saturation temperature at atmospheric condition. Initially, the entire system, including the rod heater and the inside of the tank were cleaned and the test solution was introduced. The vacuum pump is then turned on and the pressure of the system is kept low approximately below 10 kPa for 5 hr to allow all the dissolved gases to be stripped away from the test solution. Following this, the auxiliary heater was switched on and the temperature of the system was allowed rising to the saturation temperature (P=1atm). This procedure leads to obtaining a homogeneous condition throughout.

In the next step, the rod heater was heated with maximum power. This point should be highlighted that from this stage on, auxiliary heater is not used and it is switched off. After the system reached the steady state, significant data including surface temperature and visual information were recorded. The information was gathered by decreasing the

power in various intervals and recording the measurements upon reaching the steady state. Some runs were repeated two or even three times to ensure the reproducibility of the experiments.

The measured data included A) Wall temperature: this parameter was calculated based on the recorded temperatures of the thermocouples inside the rod heater and by the application of Eq. (9). The arithmetic averages of four thermocouples were assigned to the actual wall temperature, B) Bubble departing frequency: The individual bubble nucleation sites were monitored in the slow-replay of the visual information. For given nucleation site, the bubble departure frequency has been calculated by division of the counted departed bubble of the site to the time. The arithmetic average frequencies of various nucleation sites (10-20 nucleation sites at any film) were assigned to the bubble departing frequency.

2.3. Test fluids and range of parameters

In this investigation, several pure liquids have been used including: (1) water, (2) ethanol, (3) methanol, for the following reasons:

a) Distilled water, methanol and ethanol were used to check the accuracy of the experimental results and the calibration of the system for two reasons: (1) the physical properties of these are well known with high accuracy, (2) pool boiling heat transfer coefficient of distilled water and the related bubble dynamics has been studied by several investigators over a wide range of heat fluxes. The range of operating conditions used in this investigation and some selected physical properties are presented at Table 2. All the physical properties of the fluids and their boiling point (P = 1atm) data prepared from well-known handbooks [23-25]. In this study have been used ethanol and methanol of Merck's brand with 99.9% and 99.8% purity respectively.

3. Uncertainty prediction

Experimental measurements always involve uncertainties, and a systematic error analysis is useful in assessing the scatter in the data and identifying the source of any abnormal error. In the present study, uncertainties in the calculation of parameters were determined according to the single sample error propagation method outlined by Moffatt [25].

Table 2. Operating parameter and physical properties

Rang of operating parameter			
Heat Flux	5 – 115 $kW.m^{-2}$		
Physical properties at P= 1 atm			
System	Water	Ethanol	Methanol
$\mathbf{T_{sat}}$ ℃	100	78.4	64.7
$\boldsymbol{\sigma}$ $(\mathbf{Nm^{-1}})$	0.05892	0.017395	0.01889
$\mathbf{c_{pl}}$ $(\mathbf{Jkg^{-1}K^{-1}})$	4236	3126	2824
$\mathbf{k_l}$ $(\mathbf{Wm^{-1}K^{-1}})$	0.679	0.154	0.189
$\boldsymbol{\rho_l}$ $(\mathbf{kgm^{-3}})$	958.4	734.76	749.82
$\boldsymbol{\rho_v}$ $(\mathbf{kgm^{-3}})$	0.57 - 0.59	1.54 - 1.59	1.56 - 1.6
$\mathbf{h_{fg}}$ $(\mathbf{Jkg^{-1}})$	2257700	848400	1089000

This method for single-sample experiments involves the estimation of overall uncertainty δR in the calculated result R from the following relationship:

$$\delta R = \left(\sum_{i=1}^{n} \left(\frac{\partial R}{\partial X_i} \delta X_i \right)^2 \right)^{0.5} \quad (2)$$

Where R is expressed as:

$$R = R(X_1, X_2, ..., X_i, ..., X_n) \quad (3)$$

The uncertainty associated with heat transfer surface area $(A = \pi DL)$, heat flux $(q = IV/A)$, heat transfer coefficient $(h = \frac{q}{\Delta T})$ and bubble departure frequency $(f = \frac{N_b}{t})$ are calculated as:

$$\delta A = \left((\frac{\partial A}{\partial D} \delta D)^2 + \left(\frac{\partial A}{\partial L} \delta L \right)^2 \right)^{0.5} \quad (4)$$

$$\delta q = \left((\frac{\partial q}{\partial I} \delta I)^2 + \left(\frac{\partial q}{\partial V} \delta V \right)^2 \right)^{0.5} \quad (5)$$

$$\delta h = \left((\frac{\partial h}{\partial q} \delta q)^2 + \left(\frac{\partial h}{\partial \Delta T} \delta \Delta T \right)^2 \right)^{0.5} \quad (6)$$

$$\delta f = \left((\frac{\partial f}{\partial N_b} \delta N_b)^2 + \left(\frac{\partial f}{\partial t} \delta t \right)^2 \right)^{0.5} \quad (7)$$

Table 3 shows the measurement uncertainty in experimental parameters.

Table 3. Measurement uncertainty in experimental parameters

Parameter	Instrument	Range/Nominal value	Uncertainty (Δ)
Surface temperature (K)	K-type thermocouple	$69.9-111.8^{\circ}C$	$\pm 1^{\circ}C$
Bulk temperature (K)	Pt-100 thermo-resistance	$64.7, 78.34, 100^{\circ}C$	$\pm 1^{\circ}C$
Current (I)	Mastech MS8205C multi-meter	$0.9-3.5$	$\pm 0.1A$
Voltage (V)	Mastech MS8205C multi-meter	$40-220$	$\pm 1v$
Diameter (mm)		22	±0.01
Length (mm)		100	±0.01
Surface area (m^2)		0.006912	±0.047%
Heat flux ($W\ m^{-2}$)		5335−110862	11.1−2.9%
Heat transfer coefficient ($W.m^{-2}\ K^{-1}$)		966.72−9515.3	21.1−0.78%
Time (ms)		510−1830	$0.06(ms)$
Bubble departure frequency (s^{-1})		9−184	5.5−0.7%

4. Results and discussion

Fig. 3 shows heat transfer coefficients for pure liquids as a function of heat flux for system pressure of 101 kPa. The experimental data for pure water, methanol and ethanol are compared with the predictions of correlation suggested by Stephan and Abdelsalam [26] expressed as:

$$h = 0.23(\frac{k_l}{d_b})[\frac{q\,d_b}{k_l T_s}]^{0.674}\left[\frac{\rho_v}{\rho_l}\right]^{0.297}\left[\frac{h_{fg}d_b^2}{\alpha_l^2}\right]^{0.371}\left[\frac{\alpha_l^2\rho_l}{\sigma d_b}\right]^{0.35}\left[\frac{(\rho_l-\rho_v)}{\rho_l}\right]^{-1.73} \quad (8)$$

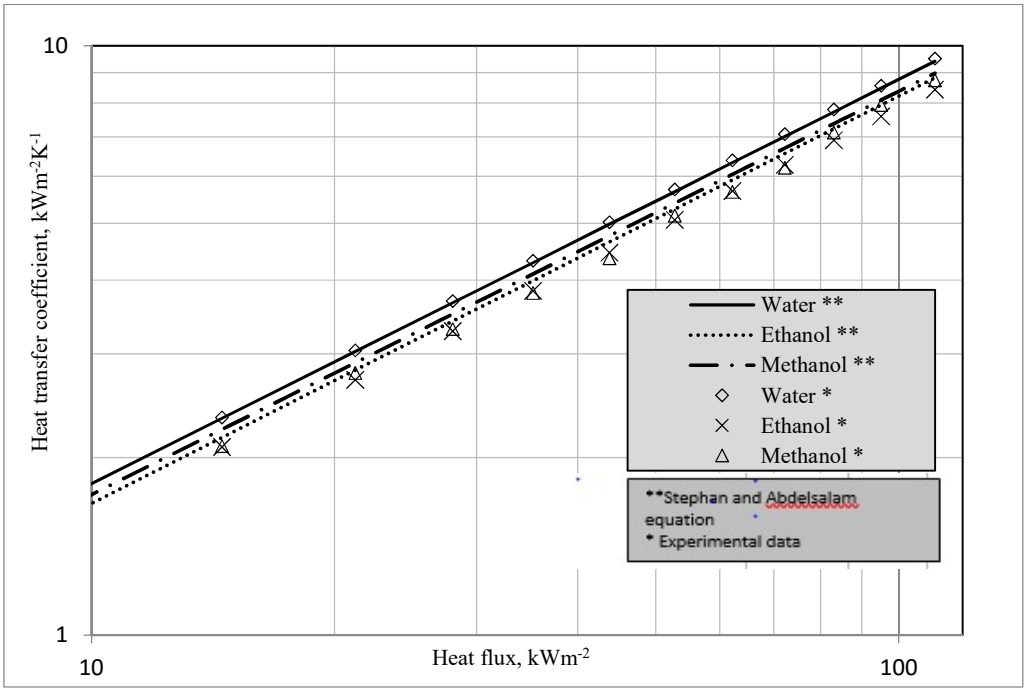

Fig. 3. Saturated nucleate pool boiling heat transfer coefficients for water, ethanol and methanol pure liquids at atmospheric pressure

Stephan and Abdel Salam [26] correlation is one of the mostly used correlations in the literature. As shown in Fig. 3 good agreement exists between the prediction and experimental data (water with an average error of approximately ±0.5%, ethanol with an average error of approximately ±4% and methanol with an average error of approximately ±5.5%). In addition, the heat transfer coefficient increases with increasing heat flux for all test fluids. It is due to the fact that an increase in boiling heat flux, in the heat flux range of this investigation, is accompanied by an increase in both number of active nucleation sites and frequency of bubble emission. The bubble behaviors pictures were obtained for pure water, ethanol and methanol at conditions of heat fluxes from 5.3 to 110.8 kW.m^{-2} and pressure of 101.325 kPa. As shown in Fig. 4 and 5, it can be found that bubble size increases with increasing heat flux.

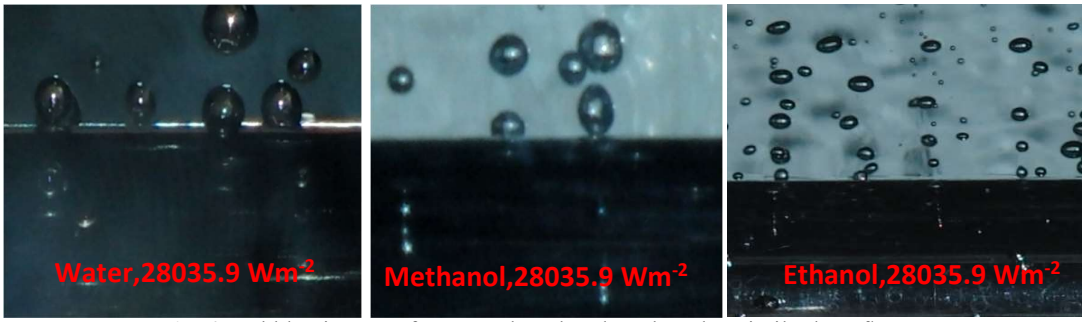

Fig. 4. Bubble pictures of water, ethanol and methanol at similar heat fluxes

The bubble departure diameters of ethanol and methanol are almost equal (1.11DAverage-Ethanol≈DAverage-Methanol (Uncertainty for bubble diameter: 0.7%)), the other models have shown this as well and are smaller than those of water at same conditions. It seems that this can result from the physical properties of test fluids especially surface tension. Water has higher surface tension than ethanol and methanol. Therefore, larger bubbles must be appeared on the heat transfer surface during the boiling of water, and more interestingly, ethanol with almost equal surface tension to methanol has equal bubble diameters. Within the range of experimental conditions of this research, Fig. 6 shows the bubble departure frequency of water, ethanol and methanol as a function of heat flux.

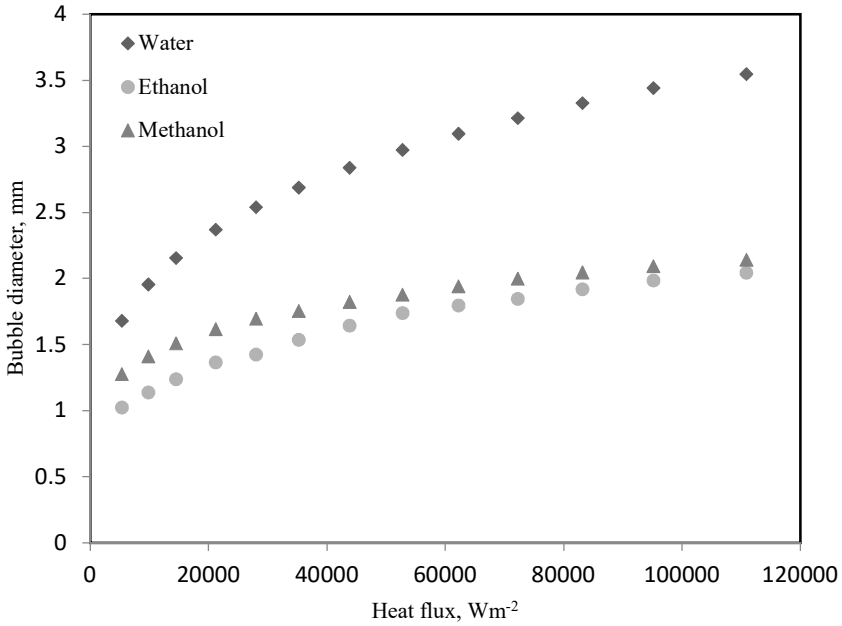

Fig. 5. Bubble diameter of water, ethanol and methanol at various heat fluxes

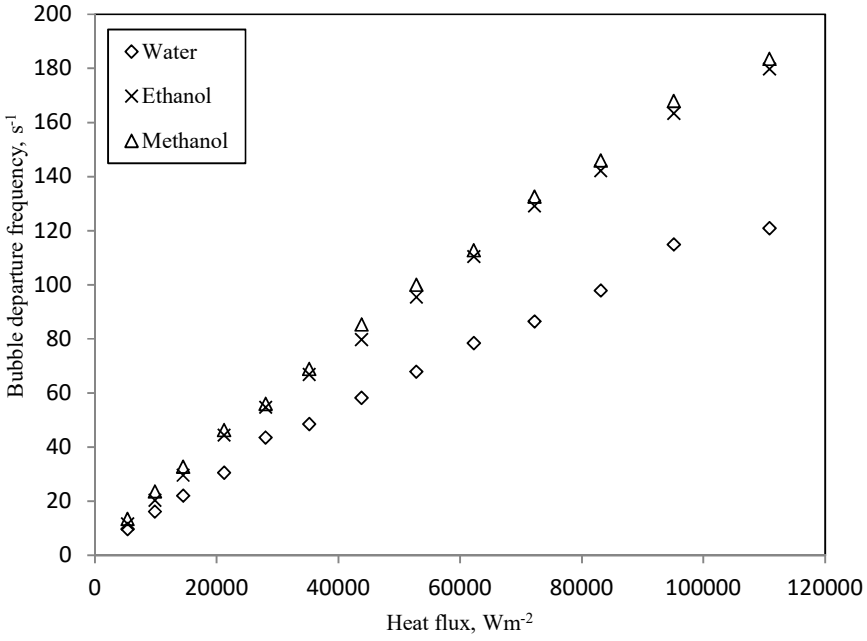

Fig. 6. Bubble departure frequency (water, ethanol and methanol)

The data show that bubble departure frequency increases by increasing heat flux, i.e. increase in wall superheat, for all test fluids. This phenomenon can be due to increase in the rate of bubble generation, i.e. reduction in the waiting time and growth time. Fig. 7 compares the predictions of various bubble departure frequency correlations with the measured departure frequencies in the current study. Note that, as shown in this figure, the various bubble diameter correlations and experimental data of this study have been used for prediction of the bubble departure diameter parameter at bubble frequency models.

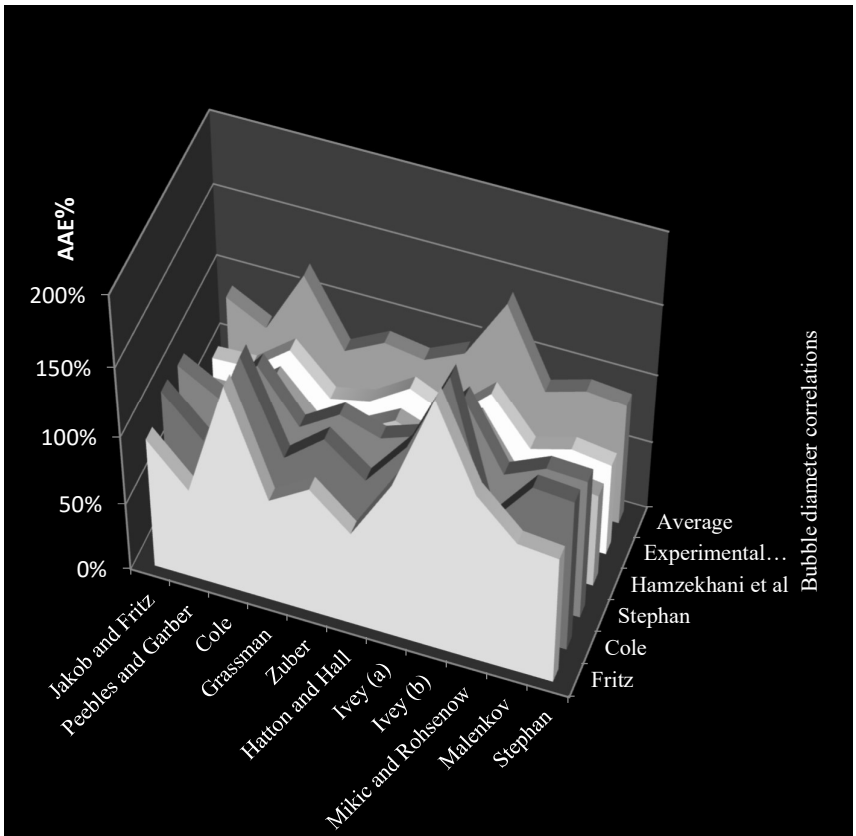

Bubble frequency correlations

	Jakob and Fritz	Peebles and Garber	Cole	Grassman	Zuber	Hatton and Hall	Ivey (a)	Ivey (b)	Mikic and Rohsenow	Malenkov	Stephan
Fritz	96%	66%	150	76%	93%	69%	113	183	123	97%	94%
Cole	108	80%	149	84%	106	84%	117	176	80%	114	112
Stephan	104	88%	121	84%	101	92%	102	138	91%	104	103
Hamzekhani et al	67%	66%	89%	60%	67%	82%	72%	99%	58%	72%	68%
Experimental data	65%	66%	87%	59%	66%	83%	71%	96%	63%	71%	68%
Average	88%	73%	119	73%	87%	82%	95%	138	83%	92%	89%

Fig. 7. Comparison of the performance of different correlations for the bubble departure frequency with experimental data

The absolute average error is defined by Eq. (9):

$$AAE\,\% = \left[\frac{x^{\,predicted}}{x^{\,\mathrm{experimental}}} - 1 \right] \times 100 \tag{9}$$

In regard to Fig. 7, using Hamzekhani et al.'s [22] model for bubble departure diameter, Mikic and Rohsenow's [19] has the best overlapping with the experimental data. However, there is a relatively large deviation between experimental data of bubble departure frequency and prediction models. Following reasons can be considered as factors for this deviation. Most proposed models for bubble departure frequency include the parameter of bubble diameter. On one hand, on the basis of the experimental results and the predicting models for bubble departure diameter (For example: Cole [15]), bubble departure diameter increases by increase in heat flux; on the other hand, there is a reverse correlation between bubble departure diameter and bubble departure frequency in the some predicting bubble departure frequency models (For example: $fd = 0.078$ [11], $f\,d_b^{0.5} = 0.9g^{0.5}$ [18]. Hence, the results of these predicting models for bubble departure frequency have a decreasing trend by increase in heat flux. But in this study, the obtained data show both bubble departure frequency and diameter increase by increase in heat flux (Fig. 5, 6). McHale and Garimella [14] have been reported the same results.

5. Conclusion

An experimental investigation on vapor bubble formation for pure water, ethanol and methanol under nucleate saturated pool boiling conditions has been performed and the experimental results indicated heat transfer coefficient increases with increasing heat flux for all test fluids at the experimental condition. It is because of the fact that an increase in boiling heat flux, in the heat flux range of this investigation, is accompanied by an increase in both number of active nucleation sites and frequency of bubble emission. Bubble diameter increases with increasing heat flux for all test fluids. Most predictions have a similar trend for increasing bubble diameter versus increasing heat flux. Bubble departure frequency increases with increasing heat flux for all test fluids. Increase in the rate of bubble generation, reduction in the waiting time and growth time can be the causes of this phenomenon.

Acknowledgements

Authors of this article would like to appreciate University of Sistan and Baluchestan for their financial and mental supports.

Nomenclature

Symbols

A	Area (m^2)
Ar	Archimedes number
A_P	Projection areas
A_r	Rough surface
Bo	Bond number
g	Growing
g_c	Correction coefficient of incompatible
h	Heat transfer coefficient (W m^{-2} K^{-1})
h_{fg}	Latent heat of vaporization (J kg^{-1})
q	Heat flux (W m^{-2})
T	Temperature (K)

Greek symbols

α	Thermal diffusivity (m^2 s^{-1})
ρ	Density (kg m^{-3})
σ	Surface tension (N m^{-1})
Δ	Difference
μ	Dynamic viscosity (Pa s)

Subscripts

b	Bubble
c	Cavity
l	Liquid
sat	Saturation
v	Vapor

V	Velocity (m s^{-1}) / Voltage (V)	*lv*	Liquid-vapor
I	Electrical current (A)	*w*	Waiting
k	Thermal conductivity coefficient (W m^{-1} K^{-1})		
N_b	Number of departed bubbles of given site		
t	Time (s)		

References

[1] Alavi Fazel, S. A., Shafaee, S.B., 2010. Bubble dynamics for nucleate pool boiling of electrolyte solutions. ASME. J. Heat Transf. 132(8), 825021-7. http://doi.org/ 10.1115/1.4001315

[2] S. Hamzekhani, M. Maniavi Falahieh, M.R. Kamalizadeh, Z. Nazari,.2015. Experimental study on bubble departure frequency for pool boiling of water/NaCl solutions. International Journal of Heat and Mass Transfer. 51, 1313–1320. http://doi.org/ 10.1007/s00231-015-1502-x

[3] Jamialahmadi, M., Helalizadeh, A., Müller-Steinhagen, H.M., 2004. Boiling heat transfer to electrolyte solutions. Int. J. Heat Mass Transfer. 47,729-742. http://doi.org/10.1016/j.ijheatmasstransfer.2003.07.025

[4]. Choi, G., Shim, D.I., Lee, D., Kim, B.S., Cho, H.H., 2019. Enhanced nucleate boiling using a reduced graphene oxide-coated micropillar, International Communications in Heat and Mass Transfer,109,104331. http://doi.org/10.1016/j.icheatmasstransfer.2019.104331

[5] Khooshehchin, M., Mohammadidoust, A., Ghotbinasab, S., 2020, An optimization study on heat transfer of pool boiling exposed ultrasonic waves and particles addition, International Communications in Heat and Mass Transfer, 114, 104558. http://doi.org/10.1016/j.icheatmasstransfer.2020.104558

[6] Hamzekhani, S., Sardashti Birjandi, M.R., Shahraki, F., 2022. Modeling and Optimization of the Bubble Detachment Diameter for a Pool Boiling System, Chem. Eng. Technol, 45, 1036–1047. http://doi.org/10.1002/ceat.201900640

[7] Sarafraz, M.M., Kiani, T.,Hormozi, F., 2016.Critical heat flux and pool boiling heat transfer analysis of synthesized zirconia aqueous nano-fluids. International Communications in Heat and Mass Transfer,70, 75-83. http://doi.org/10.1016/j.icheatmasstransfer.2015.12.008

[8] Kim, J., Oh, B.D., Kim, M.H., 2006. Experimental study of pool temperature effects on nucleate pool boiling. Int .J. Multiphase Flow, 32, 208–231. http://doi.org/ 10.1016/j.ijmultiphaseflow.2005.09.005

[9] Gorenflo, D., Chandra, U., Kotthoff, S., Luke, A., 2004. Influence of thermo physical properties on pool boiling heat transfer of refrigerants, Int. J. Refrigeration. 27, 492-502. http://doi.org/ doi.org/10.1016/j.ijrefrig.2004.03.004

[10] Gorenflo, D., Baumhogger, E., Herres, G., Kotthoff, S., 2014. Prediction methods for pool boiling Heat Transfer: A state-of-the-art Review, International Journal of Refrigeration. 43, 203-226. http://doi.org/10.1016/j.ijrefrig.2013.12.012

[11] Kim, J., Kim, M.H., 2006. on the departure behaviors of bubble at nucleate pool boiling, International Journal of Multiphase Flow. 32, 1269–1286. http://doi.org/10.1016/j.ijmultiphaseflow.2006.06.010

[12] Peebles, F.N., Garber, H.J., 1953. Studies on motion of gas bubbles in liquids, Chem. Eng. Prog. 49, 88–97.

[13] Zuber, N., 1963. Nucleate boiling the region of isolated bubbles similarity with Natural Convection, Int. J. Heat Mass Transfer. 6, 53–65. http://doi.org/ 10.1016/0017-9310(63)90029-2

[14] McHale, J.P., Garimella, S.V., 2010. Bubble nucleation characteristics in pool boiling of a wetting liquid on smooth and rough surfaces, International Journal of Multiphase Flow, 36, 249–260. http://doi.org/ 10.1016/j.ijmultiphaseflow.2009.12.004

[15] Cole, R. 1967. Bubble frequencies and departure volumes at subatmospheric pressures, AICHE J. 13, 779-783. http://doi.org/10.1002/aic.690130434

[16] Hatton, A.P., Hall, I.S., 1966. Photographic study of boiling on prepared surfaces, in: Third International Heat Transfer Conference. Chicago, pp. 24 –37. http://doi.org/10.1615/IHTC3.1130

[17] McFadden, P.W., Grassman, P., 1962. The relation between bubble frequency and diameter during nucleation pool boiling, International Journal Heat Mass Transfer. 5. 169-173. http://doi.org/10.1016/0017-9310(62)90009-1

[18] Ivey, H., 1967. Relationships between bubble frequency, departure diameter and rise velocity in nucleate boiling, International Journal Heat and Mass Transfer. 10, 1023-1040. http://doi.org/10.1016/0017-9310(67)90118-4

[19] Mikic, B.B., Rohsenow, W.M., 1969. Bubble growth rates in non-uniform temperature field, progress in Heat and Mass Transfer. 2, 283-293. http://doi.org/10.1016/0017-9310(70)90040-2

[20] Malenkov, I.G., 1971. Detachment frequency as a function of size of vapor bubbles, Translated Inzh. Fiz. Zhur. 20, (99).

[21] Stephan, K., 1992. Heat transfer in condensation and boiling,Springer, NewYork.

[22] Hamzekhani, S., Maniavi Falahieh, M., Akbari, A., 2014. Bubble departure diameter in nucleate pool boiling at saturation: Pure liquids and binary mixtures. International Journal of Refrigeration. 46, 50–58. http://doi.org/ 10.1016/j.ijrefrig.2014.07.003

[23] Daivid, R. L., 2004. Handbook of chemistry and physics, 84th. CRC Press LLC.

[24] Perry, R.H., Green, D.W., 1999. Perry's Chemical Engineering Handbook, seventh ed. MCGraw Hill, New York.

[25] Moffatt, R.J., 1988. Describing the uncertainties in experimental results, Experimental Thermal and Fluid Science, 1, 3-17.

[26] Stephan, K., Abdelsalam, K., 1980. Heat transfer correlation for boiling, International Journal of Heat and Mass Transfer. 23(1), 73-87. https://doi.org/10.1016/0017-9310(80)90140-4

[27] Fritz, W., 1935. Berechnung des Maximalvolumens von Dampfblasen ed. Phys. Z. 36, 379-384.

[28] Cole, R., Rohsenow, W.M., 1966. Correlation of bubble departure diameters for boiling of saturated liquids, Chemical Engineering Progress Symposium series, 65,211–213.